

The effects of spatial variability of mechanical parameters on a 3D landslide study

A. Pasculli, M. Calista & M. Mangifesta

Department of Geo-Technology, University of Chieti-Pescara, Chieti, Italy

ABSTRACT: In the framework of numerical modeling of landslide triggering and evolution, two important issues, among others, must be addressed. One is about a reasonable reconstruction of local and global geometry of the involved geological structures of the system. The other one, with which we are mainly concerned in this paper, regards the problem of how to satisfactorily handle the spatial variability of important parameters related to the selected constitutive models. Thus, in order to explore the importance of different spatial distribution values of mechanical parameters on landslide numerical studies, we applied a methodology based on random number generation, already proposed by one of the authors, to carry out about fifty-three *FLAC*^{3D} runs of the same model of an actual landslide. For each run, different sets of numerical values for the selected parameters have been automatically implemented. Finally some statistical considerations have been reported.

1 INTRODUCTION

The numerical experiments discussed in this paper have been applied to an actual landslide located in central Italy. In particular we studied the cinematic evolution of a travertine plate on a clay substratum, characterizing the territory of Roccamontepiano (Abruzzo Region). Some sample laboratory tests have been carried out to define physical and mechanical parameters of lithotypes and their numerical variability. The landslide modeling has been performed with *FLAC*^{3D} (Itasca 2000). Both statistical and probabilistic approaches provide the numerical modeling of complex phenomena, like landslides, with powerful tools in order to include, in some way, the inevitable spatial heterogeneities. Therefore, in this paper we adopted a methodology to assign, in a reliable random way, the supposed values of the mechanical parameters to each node of the numerical grid. More than fifty-three runs have been carried out, considering each time a different value of some selected parameters, extracted randomly among the “ensemble” of all the possible “realizations” of the statistic, assumed to be Gaussian, to which the set of the numerical values of the considered parameters have been supposed to belong. The soil was simulated with the *elastic-perfectly-plastic* model with failure being described by a composite *Mohr-Coulomb criterion* with a tension cut-off, implemented by default in *FLAC*^{3D}. The stability analyses have been performed considering the strength reduction factor (*SRF*) technique through

the non-convergence of the *maximum unbalanced force*, partially compared with the *nodal displacement method (NDM)*.

Comparison of the results obtained by averaged mechanical parameters with the results obtained by random realizations is discussed as well.

Then to analyze how much each single spatial mesh was close to its failure condition, a stress distance, from its Mohr-Coulomb failure line in the principal stresses plane, which we named *strength failure indicator (SFI)*, was introduced. The set of all *SFI* values formed, for each run, an ensemble with an arithmetic mean, characteristic for each of the six sectors in which the landslide area has been divided. A statistical analysis of the *SFI* parameter of each sector was discussed in order to introduce a *numerical landslide micro-zonation* concept. Further, in each sector, a linear correlation coefficient among the values of soil mass in plasticity state and the *SRF* calculated for the whole set of runs, have been introduced.

2 GEOLOGICAL SETTING

The selected area is localized at the border between two little villages, Roccamontepiano and Seramonacesca, on the eastern piedmont strip of the Maiella massif in Abruzzo (Italy).

The main characteristic of this area (Crescenti et al. 1987) called Montepiano is the presence of a travertine plateau, which dominates both topographi-

cally and morphologically the sequence of the hilly landforms below. The plateau shape is sub rectangular and extends itself towards the Apennine direction. Its maximum length is about 2.3 km (along the NW-SE direction) and its maximum width is about 0.7 km. Its altitude ranges from 610 to 650 meters about the sea, slightly inclined towards the NE. The edges of this travertine plate have been subjected to widespread landslide activity. In the past it has caused particularly dangerous events, such as the one that occurred in June 1765, which destroyed the built up areas. As a consequence, the relief is almost completely surrounded by detrital bodies, some very big, which characterize most of the south territory of Roccamontepiano village. The eastern sectors are characterized by smooth hilly relief and are constituted essentially of clayey sandy Plio-Pleistocene sediments (see the geological map, 1:5000 scale, reported in Fig. 1)

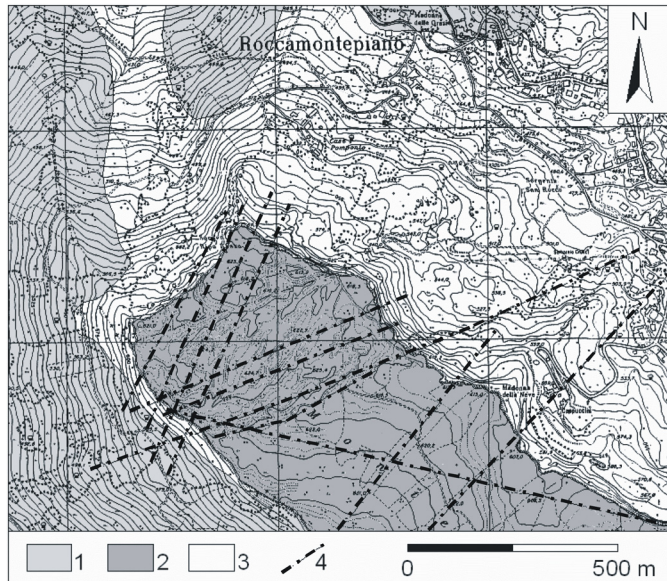


Figure 1. Geological map of Montepiano's area: 1) clayey lime; 2) Travertine; 3) landslide detritus; 4) fractures.

3 PHYSICAL MODEL RECONSTRUCTION

In order to specify the main lithological units of the entire area, the first step was a detailed geologic survey. The selected area shows some continental deposits which are characterized also by important geometry and thickness variability. Therefore, it was necessary to carry out some geophysical surveys. In particular vertical geo electrical methodologies have been applied, through different inter-electrodes distances in order to follow the contact, localized at different depths, between continental formation and the clay below. This kind of survey has been calibrated with continuum logs realized in the same area. Overlapping the data from both types of surveys, a satis-

factory physical model, in particular of the travertine plate, was obtained.

Finally, laboratory tests have been performed to define some of the most important mechanical parameters and their variability (see Table 1).

Table 1. Mechanical parameters from laboratory tests.

	Travertine		Clay	
	min	max	min	max
Unit weight (γ) (Kg/m ³)	2000	2400	2000	2100
Friction Angle (ϕ) (°)	35	45	23	24
Young Mod. (E) (GPa)	4	10	0.05	0.36
Cohesion (c) (kPa)	0	200	10	35

4 *FLAC*^{3D} MODEL RECONSTRUCTION

Particular care was taken to build up the 3D numerical modeling of the selected area through the topographical map, completely digitized by a fine kriging interpolation (3 × 3 meters square meshes), the geological map and the geophysical surveys. Given the large model dimension and the lithological complexity, only two different types of material have been assumed: travertine, which included all the related lithotypes (debris, travertine sands and so on) and clay in which surface covering has been considered.

The next step was the reconstruction, in particular by geo electrical methods, of the contact between travertine and clay. Only the northern sector of the relief area has been modeled since stability problems are localized in these zones. The related volume, selected in order to carry out numerical experiments, was 1400 meters wide, 1000 meters long and about 250-450 meters high. A numerical grid was built of more than 47,000 tetrahedrons whose largest dimension was of 10 meters at the surface and up to 40 meters in depth. Among the different constitutive models available in *FLAC*^{3D}, the Mohr-Coulomb failure criteria have been selected.

5 SPATIAL HETEROGENEITY

Among the types of physical and structural heterogeneities, only spatial variability due to lithostatic load and local uncertainty of the parameter values has been employed in the numerical experiments discussed in this paper. In particular the fractures of the travertine plateau (see Fig.1) will be included in the next modeling improvements. The usual procedure in numerical modeling implies the assignment of averaged values of mechanical parameters to each lithotype layer. In a non-linear condition it is debatable if this kind of approach may or may not provide conservative results with respect to actual values (Kaggwa 2000). Thus, in the literature, in order to

include the inevitable spatial variability, several methodologies have been discussed, but usually they are based on the following equation:

$$Phys(\mathbf{P}) = \mu(\mathbf{P}) + \delta \quad (1)$$

where $Phys(\mathbf{P})$ is the random parameter at the point \mathbf{P} , $\mu(\mathbf{P})$ is the averaged value of the selected parameter and δ is the random perturbation usually assumed as a Standard Gaussian. In this paper, however, we adopted a simplified 3D version of a 2D approach particularly suitable for granular soils (Pasculli & Sciarra 2002a,b) and implemented in $FLAC^{3D}$ through the FISH program. In this model the selected parameters $Phys(\mathbf{P})$ are assumed to be the result of two physical causes: the first one is supposed to be due to the random formation of the granular deposit layer, while the second one is supposed to be due to a stochastic force, around a deterministic trend. The second term, which we call *stochastic-deterministic constraint (SDC)*, is supposed to include all the mechanical influence of the system on the soil element around the point \mathbf{P} . The difference with the more common approach (Eq. 1) is that the stochastic character of the phenomena is not imposed by a simple mathematical term (δ), but it is, in some way, justified by a physical point of view. Thus the following equation has been employed:

$$Phys(\mathbf{P}) = Phys_r(\mathbf{P}) + [\mu(\mathbf{P}) - Phys_r(\mathbf{P})] \times [mean + \sigma \times G_norm] \times \exp\left\{-[f(\mathbf{P})/s]^2\right\} \quad (2)$$

where $Phys(\mathbf{P})$ was again the random parameter (Young Modulus, friction angle, cohesion, bulk unit weight and so on) at the point \mathbf{P} ; $Phys_r(\mathbf{P})$ was the value due to the random formation of the selected soil layers; $\mu(\mathbf{P})$ was the deterministic trend of the *SDC*. While the term $[mean + \sigma \times G_norm]$ was a non-dimensional number related to the random factor of the exerted *SDC*, in which “mean” was the average term, σ the standard deviation and G_norm the standard Gaussian distribution. The last factor $\exp\left\{-[f(\mathbf{P})/s]^2\right\}$ has been introduced to include weakness and perturbations (just like fractures, for example), localized along curves or geometrical zones described by the $f(\mathbf{P})/s$ function. The ratio $f(\mathbf{P})/s$ weighs how far the considered point \mathbf{P} is from the curve $f(\mathbf{P})$. In fact if the point lies along the curve, it follows that $f(\mathbf{P})=0$ and the term $\exp\left\{-[f(\mathbf{P})/s]^2\right\}$ is equal to its maximum value. For all the numerical experiments discussed in this paper, $\exp\left\{-[f(\mathbf{P})/s]^2\right\} = 1$ has been assumed. Further, the variable G_norm has been supposed to be a standard Gaussian distribution provided by the Box & Muller (1958) algorithm:

$$G_norm = \sqrt{[-2\ln(y_ran1)]} \times \cos(2\pi \times y_ran2) \quad (3)$$

where y_ran1 and y_ran2 were two non-correlated (pseudo) random variables uniformly distributed in the interval (0,1) and provided directly by the FISH

function, URAND. Moreover, for the sake of simplicity, spatial correlation of mechanical parameters has not been employed.

6 MECHANICAL PARAMETERS

Essentially only travertine and clay materials have been included. The bulk unit weight of the materials has been selected as the random variable, while the other parameters have been employed as a linear function of it, in such a way as to save their variability through the numerical range provided by laboratory tests and reported in Table 1. For all the simulations, Poisson coefficient $\nu = 0.3$ has been assumed. For the travertine the bulk unit weight has been supposed to be a Gaussian variable not dependent on the depth. Thus from Equation 1, setting $mean = 0$ and $\sigma = 0$, it followed:

$$Phys(\mathbf{P}) = Phys_r(\mathbf{P}) \quad (4)$$

Then, in order to include the whole numerical range of the travertine bulk unit weight, the standard deviation has been assumed to be:

$$\sigma = (\gamma_{max} - \gamma_{mean}) / 4 \equiv 50 \quad (5)$$

In such a way more than 93% of the values of the random ensemble were included in the range reported in Table 1. Random values outside of the range have been assumed to be equal to the mean. Then we employed the following illustrative relations, related to some selected parameters, for which the symbol \mathbf{P} of the point has been omitted and on which some other parameters depend:

$$\gamma_{tr}(Kg/m^3) = 2200 + (50 \times G_norm) \quad (6)$$

$$E(Pa) = (E_{max} - E_{min}) \frac{(\gamma_{tr} - 2000)}{(\gamma_{tr_max} - \gamma_{tr_min})} + E_{min} \equiv \quad (7)$$

$$\equiv 6 \times 10^9 \frac{(\gamma_{tr} - 2000)}{400} + 4 \times 10^9$$

$$Fric_ang = \frac{(\gamma_{tr} - 2000)}{40} + 35^\circ \quad (8)$$

On the other hand, the unit weight of the clay material has been supposed to change linearly through the depth. So from Equation 1 and Table 1, and after the aforementioned discussion, the following expressions have been employed (symbol \mathbf{P} omitted again):

$$\gamma_c = \gamma_{c_r} + [\mu - \gamma_{c_r}][1 + 0.125 \times G_norm2] \quad (9)$$

$$\gamma_{c_r} = 2050 + (12.5 \times G_norm1) \quad (10)$$

where G_norm1 and G_norm2 were two Gaussian variables extracted by two different, subsequent calls to the FISH (pseudo) random routine, URAND.

The term μ was the deterministic trend of the effect of the total force exerted on the soil element, which, in this case, was supposed to be due to the lithostatic loading. The height ranges from 350 meters up to about 650 meters on the sea level. Thus the following expression was assumed:

$$\mu \equiv \mu(\mathbf{P}) = \frac{(2100 - 2000)}{[h_{max}(x, y) - 350]} \times z(x, y) + 2000 \quad (11)$$

where $h_{max}(x, y)$ was the maximum altitude of the topographic surface of the relief, and $0 \leq z \leq [h_{max}(x, y) - 350]$ was the distance of the point \mathbf{P} from the surface of the clay material. The variation law of the other parameters is assumed to follow linear trends, similar to travertine's parameters.

7 PROBABILISTIC RISK APPROACH

In order to make some quantitative consideration about the risk of local instabilities relative to a relief similar to the geological system we are concerned with, we adopted the criteria to analyze how far the local stress state is from the failure region in the principal stress plane (σ_1, σ_3) . The following Mohr-Coulomb with tensile cut-off failure criteria has been assumed (*FLAC^{3D} manual*, Itasca 2000):

$$f^s = \sigma_1 - \sigma_3 N_\phi + 2c\sqrt{N_\phi}; \quad f^t = \sigma_3 - \sigma^t \quad (12)$$

$$N_\phi = [1 + \sin(\phi)] / [1 - \sin(\phi)]; \quad \sigma^t_{max} = c / \tan(\phi)$$

Then the simplest indicative parameter, which may be introduced for this purpose, is just the distance d_i (see Fig. 2):

$$d_i = \frac{|\sigma_{1i} - \sigma_{3i} N_{\phi i} + 2c_i \sqrt{N_{\phi i}}|}{\sqrt{1 + N_{\phi i}^2}} \quad (13)$$

We called d_i the *strength failure indicator (SFI)*. Further we supposed $\sigma^t_i \equiv \sigma^t_{max i} = c_i / \tan(\phi_i)$. Due to the spatial heterogeneities, different values of ϕ_i , and c_i and a peculiar principal stress plane have been associated to each physical point. Moreover, to analyze the risk of instability at an intermediate scale, we divided the selected geological system in six 50-meter thick sectors. Finally, we carried out 53 stability analyses of the same previously described numerical model, each time with different values of mechanical parameters, provided by different random realizations of the same statistic.

As stability analysis criterion, we followed the *strength reduction factor (SRF)* technique (Matsui & Sun 1992). By means of this approach, the system was assumed to be in incipient collapse state as soon as the *maximum unbalanced force (MUF)* was going to diverge, as shown in Figure 3. Then we compared the value of the *SRF* approach obtained by one of

the simulation carried out applying the *MUF* technique with the results provided by the *nodal displacement method (NDM)* (Giam & Donald 1988).

Figure 4 shows the results obtained by applying *NDM* which allows to define, for the selected system, at least roughly, the elastic field behavior only around point A (just only few max displacement millimeters), the occurrence of local instabilities between points A and B, and finally global failure, after point B.

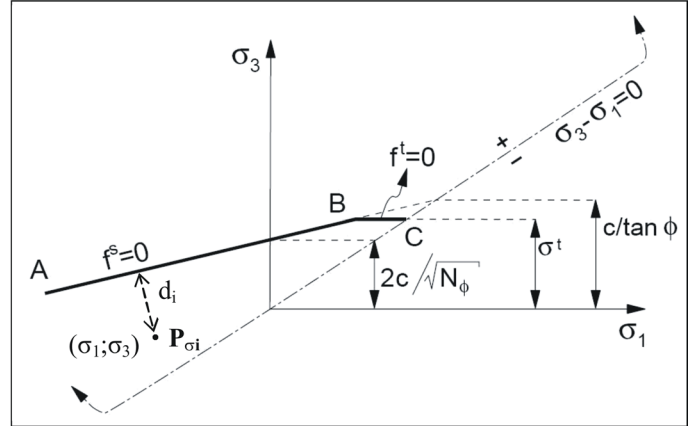


Figure 2. Principal stress plane with failure criteria associated to the point i -th.

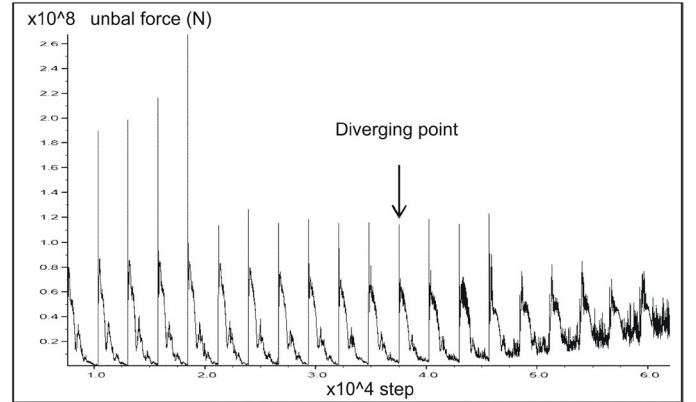


Figure 3. Maximum unbalanced force iterations.

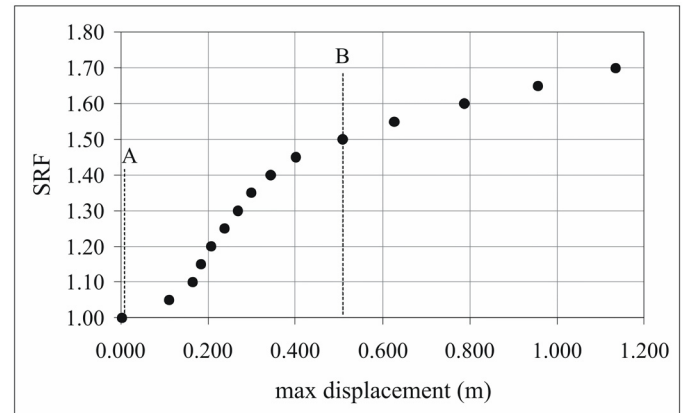


Figure 4. *SRF* vs. max nodal displacement.

The SRF value obtained by NDM approach was congruent enough with that calculated by MUF method for the selected running (Fig. 11). Then, in the framework of a numerical “*probabilistic micro zoning*” procedure related to instability risk, we introduced two simple numerical indicators, calculated for each run, related to each spatial sector in which we have divided the selected system. The first one was a plasticity ratio:

$$DI_{ik} = V_{ik} / V_{itot} \quad (14)$$

where V_{ik} was the soil mesh volume of the sector i -th in a plasticity state, obtained in the k -th running, while V_{itot} was the total volume of the i -th sector layer. The second one, calculated again for each sector, was an *averaged strength failure indicator*, weighted by means of the “importance” ratio of the volume V_j of the j -th mesh over the total volume V_{itot} of the i -th sector:

$$\mu_{di} = \frac{1}{N_i} \sum_{j=1}^{N_i} \left[d_j \frac{V_j}{V_{itot}} \right] \quad (15)$$

where N_i is the number of meshes in the i -th sector. The first indicator was related to the calculated mobilized mass for each sector and for each run, therefore related to how much the soil material inside the selected sector has been damaged. So we called it the numerical *degrade indicator* (DI). The second one specified how far the stress state of the soil material was from failure conditions. Thus we called it: numerical *hazard stress state indicator* ($HSSI$).

8 RESULTS OF ANALYSES AND STATISTICAL CONSIDERATIONS

We carried out 53 runs. Then we reported in Figure 5 the *probabilistic distribution of the strength reduction factor*: the occurrence number of the analyses for which a specific value of the SRF (*strength reduction factor*) has been provided by the simulations and their frequencies related to the total number of runs.

Figure 6 shows the view of two realizations related to the minimum and the maximum values of the SRF number, respectively equal to 1.25 and 1.6. Below, in the same figure, we have included the display of material already in plastic state whose *strength failure indicator* d_i was vanishing, in red, while, in grey, the other points. It is worthwhile to observe that for the same value of the SRF number, both different spatial displacements and plastic soil material distributions may be numerically expected (see Fig. 7, in which the max displacements ranged from 0.55 m up to 0.74 m). For this reason, in Figure 6 we have selected, by a comparison point of view, just those realizations with the maximum displace-

ments values related to the minimum $SRF = 1.25$ and to the max $SRF = 1.60$. It should be noted that by varying randomly the realization of the mechanical parameter values and their physical point assignment, roughly around the same average trend in depth, a numerical modeling like that we have proposed, may predict, through 53 runs, maximum soil displacements ranging from 0.24 m up to 0.9 m, so with a factor of almost 4!

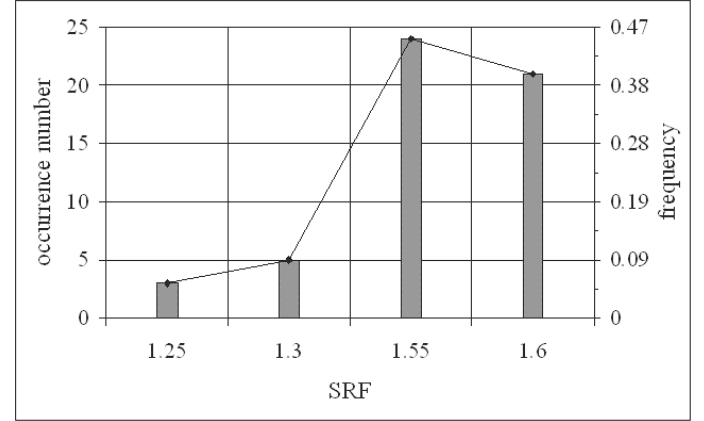


Figure 5. Probabilistic distribution of the strength reduction factor.

At this point some statistical considerations have been performed. Thus, for each sector, we analyzed the linear correlation coefficient among the total plastic soil material, expressed by the *degrade indicator* DI (Eq. 15) and the calculated SRF number:

$$r_{DI, SRF} = \frac{\sum_{j=1}^{53} (DI_j^t - \overline{DI_j^t})(SRF_j - \overline{SRF})}{53 \times \sigma_{DI} \times \sigma_{SRF}} \quad (16)$$

where DI_j^t and SRF_j were, respectively, the total plastic soil material for a specific sector and the strength reduction factor provided by the j -th run, while the others symbols were their average values and standard deviations. The coefficient $r_{DI, SRF}$ shows, by a statistical point of view, how much the selected sector was involved in the total stability occurrence.

In Figure 8 an exploded view of the sectors with their $r_{x,y} = r_{DI, SRF}$ have been sketched. By this analysis the sectors 4, 2, and 1 are the most involved. In Figure 9 we reported the occurrence number of the analyses for which a specific ratio value of the plastic soil mass, over the total mass in the selected sector (DI value) has been provided by the 53 simulations.

Thus it would be straightforward, normalizing the ordinate to the total simulation number, to obtain an estimation of the *Probability of the failed soil mass amount* in each sector. The calculated percentage of the soil in a plastic state, ranged from 1.3% up to 66%.

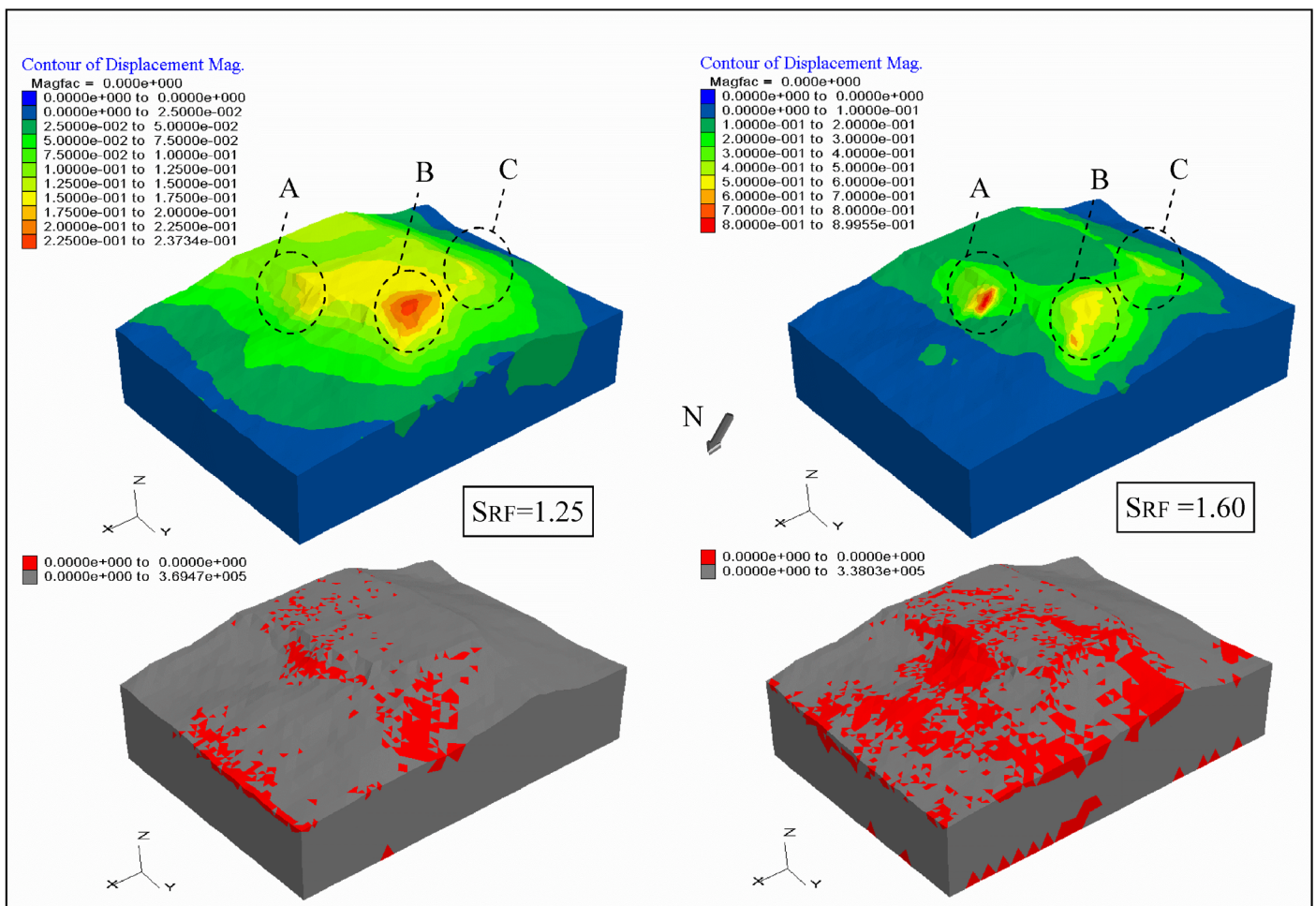


Figure 6. Displacements and plastic points plots for the two realized extreme cases.

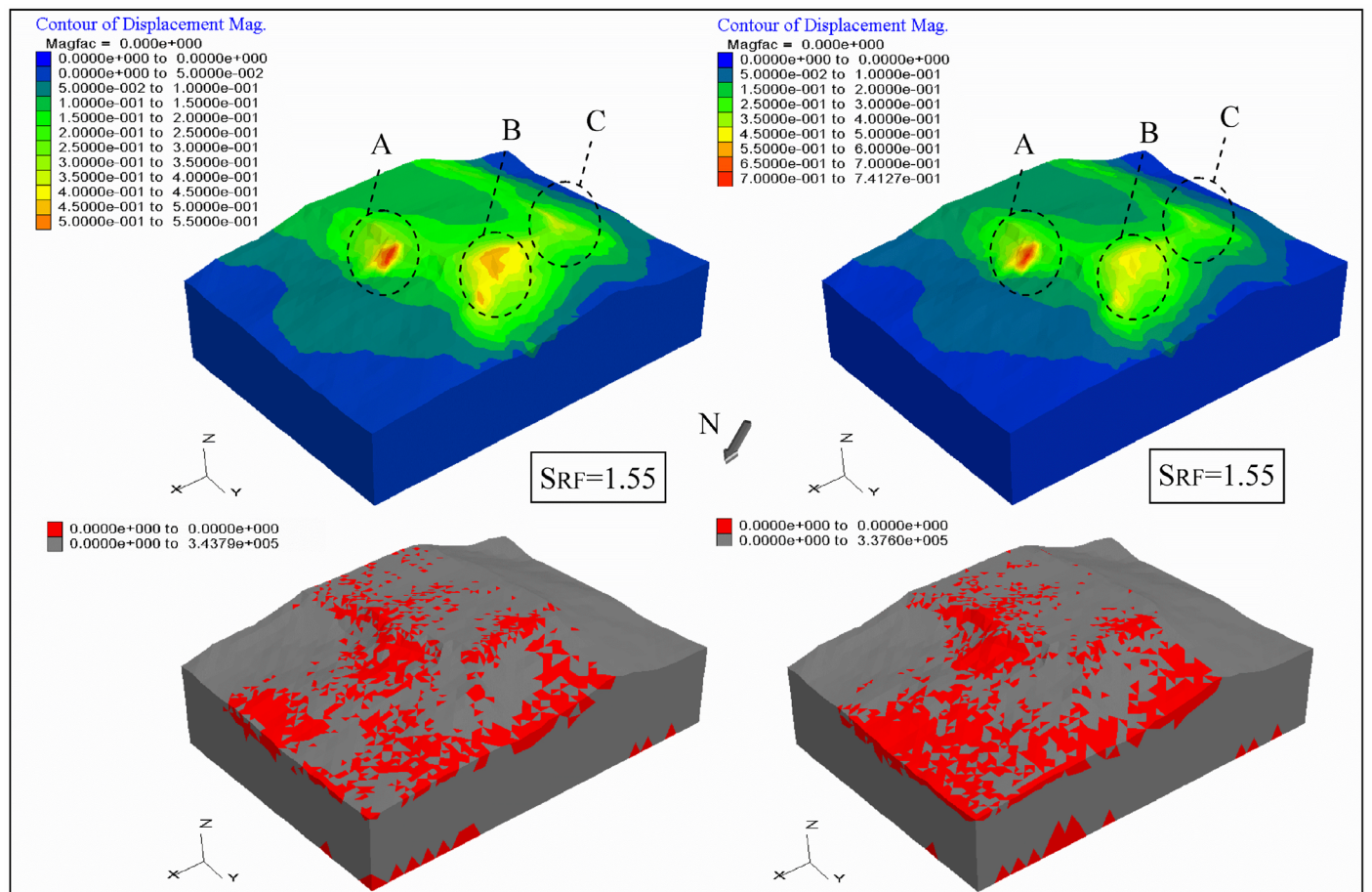


Figure 7. Comparison of the displacements and plastic points plots for the same realized *strength reduction factor*.

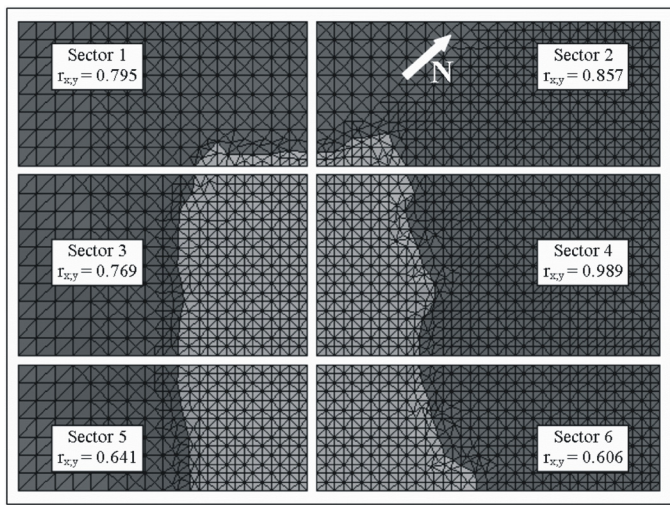


Figure 8. Sectors exploded map.

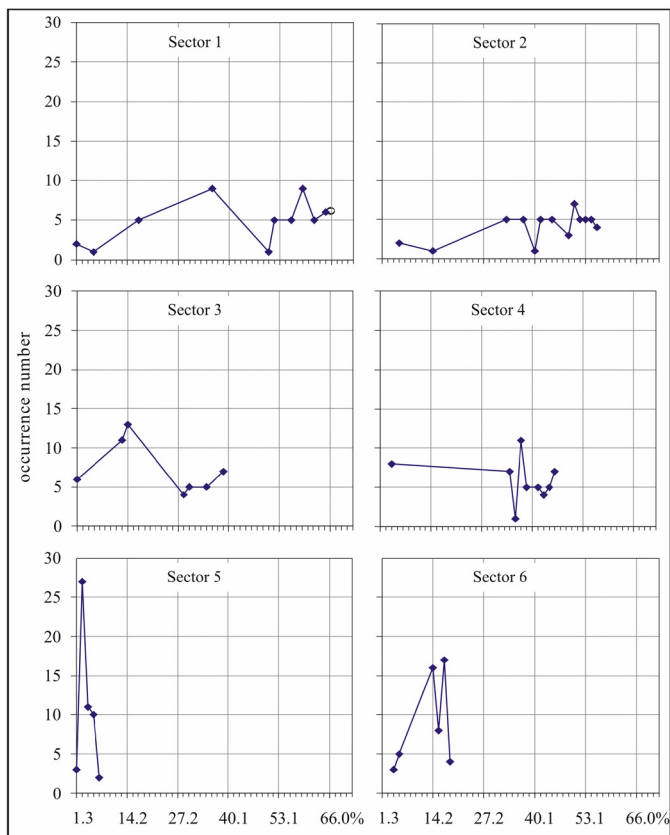


Figure 9. Occurrence number vs. percentage of the failed soil mass amount.

It is interesting to note that the effects of the selected random spatial variability have been more important for sectors 1, 2, 3, and 4. The “probability distributions” related to sectors 5 and 6 have not been so spread out along the whole range, thus these sectors have been less sensitive to the inclusion of the variability of the mechanical parameters in the modeling. Furthermore we analyzed another important parameter: the numerical *stress state hazard indicator*. Also in this case, the selected parameter μ_{di} (Eq. 15) has been calculated for each sector and for all the runs.

Due to its large numerical variability (several magnitude order), we considered its natural logarithm and then we plotted the related *occurrence number* in Figure 10. The μ_{di} parameter ranged from 0.7 kPa up to 730 kPa.

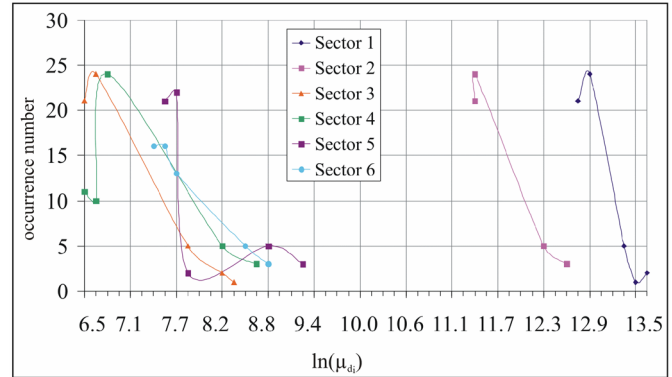


Figure 10. Occurrence number vs. natural logarithm of the stress state hazard indicator.

Finally we carried out a simulation for which the mechanical parameters have been assumed to be spatially constant and equal to their averaged values (see Fig. 11). In the actual situation, the sections labeled by ellipses A, B, and C have experienced real landslide displacement.

The results comparison of Figures 6, 7 & 11 shows that the selected modeling of spatial variability, employed and discussed in this paper, enhances the numerical values of the calculated displacement intensity and mass amount in plasticity state, with respect to a constant parameter modeling, right where landslides occurred actually.

9 CONCLUSIONS

In this paper, some numerical experiments have been applied to a study of an actual landslide. A selected modeling based on a random realization of the values of some parameter, belonging to a Gaussian statistic, has been applied in order to explore how important the influence of particular spatial variability, like those due to a specific load trend and to the local heterogeneity, is on this kind of analyses. Then the system stability and, in particular, its “*strength reduction factor SRF*” has been analyzed by means of a proposed *numerical probabilistic approach*, applied to the results of fifty-three runs of the same model.

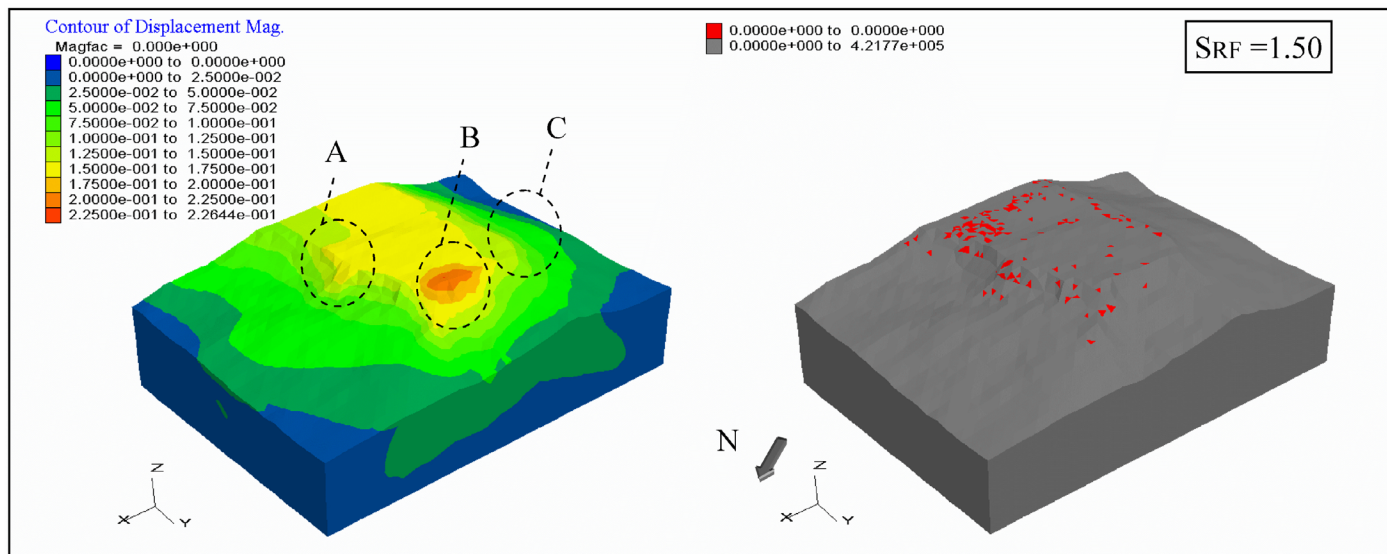


Figure 11. Displacement and plastic point plots realized with constant average mechanical parameters.

Thus, instead of being concerned with a single *strength reduction factor*, as in the usual practice, the application of this method provided a statistical distribution of the numerical values that the *SRF* number may assume. Further, in order to introduce a “micro zoning” procedure we discussed some other statistical parameters: the *degrade indicator (DI)* related to how much the soil material inside the selected sector has been damaged; the *stress state hazard indicator (SSHI)* which specifies how far the stress state of the soil material is from failure conditions. The results are quite satisfactory in comparison with the actual landslide situation.

On the other hand, we carried out another simulation considering constant mechanical parameters equal to their averaged values. These last results seem to be quite poor, enhancing the importance of handling with care, not only large-scale variability, but also small-scale heterogeneities. Although fractures have not been included in the modeling, interesting results have been realized for this particular landslide. This observation may suggest, however, that in this case the selected spatial heterogeneities and modeling have been quite enough to characterize the evolution of that particular geological system.

Future improvements will be concerned with the study of the separated effect of each kind of variability, modeling with degraded and constant parameters, inclusion of the fractures with the related random characteristic, and more statistical analyses.

ACKNOWLEDGEMENT

We would like to thank Prof. Attilio Sacripanti (ENEA) for support with the *FLAC^{3D}* runs, and Dr. Barbara Di Giandomenico for her effort in editing.

REFERENCES

- Box, G.E.P. & Muller, M.E. 1958. A note on generation of random normal deviates. *Ann. Math. Statist.* 29: 610-611.
- Crescenti, U., D'alessandro, L. & Genevois, R. 1987. Montepiano escarpment (Abruzzo, Italy): a first analysis of the geomorphologic characteristics related to stability (in Italian). *Mem. Soc. Geol. It.*, 37: 775-787.
- Itasca Consulting Group, Inc. 2000. *FLAC^{3D} – Fast Lagrangian Analysis of Continua in 3 Dimensions, Ver. 2.0 User's Manual*. Minneapolis: Itasca.
- Giam, S.K. & Donald, I.B. 1988. Determination of critical surfaces for slopes via stress-strain calculations. *Proceedings 5th Australia, New Zealand Conference in Geomechanics*, 461-464.
- Kaggwa, W.S. 2000. Determination of spatial variability of soil design parameters and its significance in geotechnical engineering analyses. In Smith & Carter (eds), *Developments in Theoretical Geomechanics*. Rotterdam: Balkema, 681-703.
- Matsui, T. & San, K.C. 1992. Finite Element slope stability analysis by shear strength reduction technique. *Soils and Foundations*, 32(1): 59-70.
- Pasculli, A. & Sciarra, N. 2002a. A 2D Mathematical and Statistical Modelling of Soils Structures. *Proceedings of 8th Annual Conference of the International Association for Mathematical Geology, September 15-20 2002 Berlin Germany*, 1, 111-116, ISSN 09468978.
- Pasculli, A. & Sciarra, N. 2002b. Nodalizzazione ed interpolazione agli elementi finiti di eterogeneità strutturali in terreni granulari. Applicazione ai pendii (in Italian). *Atti Convegno AIGA-2003*, 19-20 febbraio Chieti, ISBN 8886698402.